KUNS1675

Bifurcation of Periodic Orbit as Semiclassical Origin of Superdeformed Shell Structure *

K. Matsuyanagi †
Department of Physics, Graduate School of Science, Kyoto University,
Kyoto 606-8502, Japan

Abstract

Classical periodic orbits responsible for emergence of the superdeformed shell structure of single-particle motion in spheroidal cavities are identified and their relative contributions to the shell structure are evaluated. Fourier transforms of quantum spectra clearly show that three-dimensional periodic orbits born out of bifurcations of planar orbits in the equatorial plane become predominant at large prolate deformations. A new semiclassical method capable of describing the shell structure formation associated with these bifurcations is briefly discussed.

PACS number: 21.60.-n

1 Introduction

Regular oscillation in the single-particle level density (coarse-grained to a certain energy resolution) is called *shell structure*, and plays a decisive role in determining shapes of a finite Fermion system [1,2]. According to the periodic-orbit theory [3–7] based on the semiclassical approximation to the path integral, shell structure is determined by classical periodic orbits with short periods. A finite Fermion system (like a nucleus and a metallic cluster) favors such shapes at which prominent shell structures are formed and its Fermi surface lies in a valley of oscillating level density, increasing its binding energy in this way.

In this contribution, I would like to point out that 1) there is a unique application of the periodic orbit theory to a modern nuclear structure problem; i.e. to understand the mechanism of emergence of the *superdeformed shell structure*, and 2) bifurcation of periodic orbits is responsible for the formation of this new shell structure. It is my impression that bifurcations are often discussed in connection with "routes to chaos", but emergence of new ordered structure (in quantum spectra) through bifurcations is rarely discussed.

*To appear in the Proceedings of the Nobel Symposium "Quantum Chaos Y2K," Bäckaskog Castle, Sweden, June 13-17, 2000.

†E-mail address: ken@ruby.scphys.kyoto-u.ac.jp

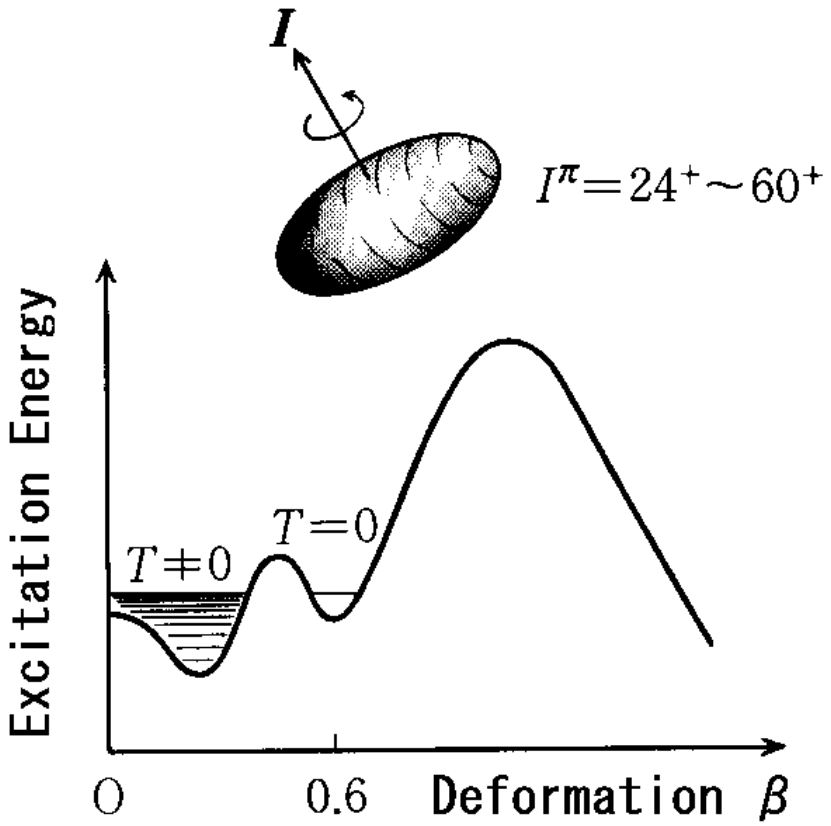

Figure 1: Illustration of the rapidly rotating superdeformed nucleus. Here T denotes the temperature, and the values of angular momentum I and parity π are those appropriate to the superdeformed band in ^{152}Dy, which was discovered in 1985 by Twin et al. [8].

2 Nuclear superdeformation

Superdeformed states are *cold* quantum states embedded in the highly excited *warm* region consisting of a huge number of compound nuclear states (see Fig. 1).

Their shapes are similar to the spheroid with the major to minor axes ratio about 2:1. Of course, when we talk about "shapes" of a finite quantum system like a nucleus, we means intrinsic shapes associated with selfconsistent mean fields. Thus the superdeformation is a striking example of spontaneous symmetry breakdown. The mean field is rapidly rotating and generates a beautiful rotational band spectrum (to restore the broken symmetry). The reason why superdeformed states can maintain their identities against compound nuclear states (whose level density is high) is that there is a barrier preventing the mixing between these different kinds of quantum states (associated with two local minima in the Hartree-Fock potential-energy surface). Therefore, in order to understand why superdeformed nuclei exist, we need to investigate the mechanism of producing the second minimum in the potential energy. It is certainly connected to an extra binding-energy gained by the formation of a new shell structure called the *superdeformed shell structure*. Our major

subject is thus to understand the mechanism how and the reason why such a new shell structure emerges. The semiclassical periodic orbit theory is useful to gain an insight into the dynamical origin of it.

3 Spheroidal cavity model

Let us consider the spheroidal cavity model as a simplified model for single-particle motions in heavy nuclei, and try to find the correspondence between quantum shell structure and classical periodic orbits. As emphasized in [6], the shell structure obtained for this model contains, apart from shifts of deformed magic numbers due to the spin-orbit potential (although they are important for realistic calculation of nuclear structure), the basic features similar to those obtained by the Woods-Saxon potential for heavy nuclei. Of course, it is necessary to examine the dependence on surface diffuseness. In fact, periodic orbits with small angular rotations between two successive reflections at the surface (like pentagons) disappear with increasing diffuseness parameter [9]. But, periodic orbits with larger angular rotations (like star-shaped orbits) survive at the realistic value of the diffuseness parameter for the nucleus [10]. Needless to say, the spheroidal cavity is a special integrable system. But, we have obtained similar results also for other parametrizations of prolate cavities (for which the Hamiltonian is non-integrable) [11]. Thus I believe that the spheroidal cavity model contains the basic features to get an insight into the problem of our primary concern; i.e. what is a proper semiclassical interpretation of the superdeformed shell structure.

In the cavity model, single-particle equations of motion are invariant with respect to the scaling transformation $(\boldsymbol{x}, \boldsymbol{p}, t) \to (\boldsymbol{x}, \alpha\boldsymbol{p}, \alpha^{-1}t)$ and the action integral S_r for a periodic orbit r is proportional to its length L_r:

$$S_r(E = p^2/2M) = \oint_r \boldsymbol{p} \cdot d\boldsymbol{q} = pL_r = \hbar k L_r. \tag{1}$$

Thus the semiclassical trace formula for the level density is written as

$$\begin{aligned} g(E) &= \sum_n \delta(E - E_n) = \frac{M}{\hbar^2 k} \sum_n \delta(k - k_n) \\ &\simeq \bar{g}(E) + \sum_r A_r(k)\, \cos(kL_r - \pi\mu_r/2), \end{aligned} \tag{2}$$

where $\bar{g}(E)$ denotes the smooth part corresponding to the contribution of the *zero-length* orbit and μ_r is the Maslov phase of the periodic orbit r. The Fourier transform $F(L)$ of the level density $g(E)$ with respect to the wave number k is written as

$$\begin{aligned} F(L) &= \int dk\, e^{-ikL} g(E = \hbar^2 k^2/2M) \\ &\simeq \bar{F}(L) + \pi \sum_r e^{-i\pi\mu_r/2} A_r(i\partial_L)\, \delta(L - L_r). \end{aligned} \tag{3}$$

By virtue of the scaling property of the cavity model, the Fourier transform exhibits peaks at lengths of classical periodic orbits, so that it may be regarded as the "length

Table 1: Bifurcation points of short periodic orbits.

orbit (p:t:q)	axis ratio (a/b)	deformation δ	orbit length in R_0
(4:2:1)	$\sqrt{2}$	0.32	7.1
(5:2:1)	1.62	0.44	8.1
(6:2:1)	$\sqrt{3}$	0.49	8.7
(7:2:1)	1.80	0.52	9.0
(8:2:1)	1.85	0.54	9.2

spectrum" [4]. In the following, we shall make use of the Fourier transforms in order to identify the most important periodic orbits that determine the major pattern of oscillations in the coarse-grained quantum spectrum.

4 Bifurcation of periodic orbit

As is well known, only linear and planar orbits exist in a spherical cavity. When spheroidal deformations occur, the linear (diameter) orbits bifurcate into those along the major axis and along the minor axis. Likewise, the planar orbits bifurcate into orbits in the meridian plane and those in the equatorial plane. Since the spheroidal cavity is integrable, periodic orbits are characterized by three positive integers (p, t, q), which represent numbers of vibrations or rotations with respect to three spheroidal coordinates. When the axis ratio η of the prolate spheroid increases, hyperbolic orbits in the meridian plane and three-dimensional (3D) orbits successively appear through bifurcations of (repeated) linear and planar orbits in the equatorial plane. Bifurcation points are determined by stability of equatorial-plane orbits against small displacements in the longitudinal direction, and bifurcations occur when the condition

$$\eta \equiv \frac{a}{b} = \frac{\sin(\pi t/p)}{\sin(\pi q/p)}. \tag{4}$$

is satisfied [4, 12], where a and b denote the lengths of the major and the minor axes, respectively. With increasing η, planar orbits (4:2:1) bifurcate from the linear orbit that repeats twice along the minor axis. With further increase of η, 3D orbits $(p{:}t{:}q) = (p{:}2{:}1)$ with $p = 5, 6, 7, \cdots$ successively bifurcate from the planar orbits that turns twice ($t = 2$) about the symmetry axis. These new-born orbits resemble the Lissajous figures of the superdeformed harmonic oscillator with frequency ratio $\omega_\perp{:}\omega_z = 2{:}1$. Every bifurcated orbit forms a continuous family of degeneracy two, which implies that we need two parameters to specify a single orbit among a continuous set of orbits belonging to a family having a common value of the action integral (or equivalently, the length).

5 Constant-action lines and Fourier transform

Figure 2 displays the oscillating part of the smoothed level density in the form of a contour map with respect to the energy and deformation parameter. Regular patterns consisting of several valley-ridge structures are clearly seen. As emphasized by Strutinsky et al. [6], if few families of orbits having almost the same values of action integral S_γ dominate in the sum in Eq. (2), the valleys in the contour map may follow such lines along which S_γ stay approximately constant. In this figure, tick solid lines running through the spherical closed shells indicate the constant-action lines for tetragonal orbits in the meridian plane. It is clear that the valleys run along these lines. A detailed discussion on this point is made in Ref. [14]. On the other hand, tick broken and solid lines in the region $\delta = 0.3 \sim 0.8$ indicate those for the five-point star shaped orbits in the equatorial plane and for the 3D orbits (5:2:1) bifurcated from them, respectively. Good correspondence is found between these lines and the valley structure seen in the superdeformed region. Constant-action lines for the other 3D orbits listed in Table 1 also behave in the same fashion.

The magnitudes of contributions of individual orbits are found to exhibit a remarkable deformation dependence. Figure 3 shows the Fourier transform of the quantum spectrum at $\delta = 0.6$ (axis ratio 2:1). We see that these 3D orbits form prominent peaks in the range $L = 8 \sim 9$. Figure 4 displays the deformation dependence of the Fourier amplitudes $|F(L)|$ defined in Eq. 3 at lengths $L = L_r$ of these orbits. We see that the Fourier peak heights associated with new orbits created by bifurcations quickly increase with increasing deformation and reach maximal values. Then, they start to decline. Thus we conclude that the bifurcations of equatorial-plane orbits play essential roles in the formation of the superdeformed shell structure, and this shell structure is characterized by the 3D orbits (p:2:1).

Some of these 3D orbits are displayed in Fig. 5. They possess similarities with the figure-eight shaped orbits in the axially symmetric harmonic-oscillator, that appear when the frequency ratio becomes exactly 2:1 [15]. It is important, however, to note a difference in that they exist in the cavity model for all deformation parameters δ larger than the bifurcation points (not restricted to the special point of axis ratio 2:1). In view of the fact that more than 200 superdeformed rotational bands have been systematically observed and they have varying deformations in the range $\delta = 0.4 \sim 0.6$ [16–18], it seems more appropriate and general to define the concept of *superdeformation* in terms of the shell structure generated by these 3D orbits (p:t:q)=(p:2:1) (rather than geometrical shapes alone).

6 Semiclassical method capable of treating the bifurcation

We have evaluated the amplitudes A in the trace formula (2) by means of the Fourier transforms of quantum spectra. Now we attempt to calculate them by semiclassical method. As is well known, however, the amplitude A evaluated by the conventional stationary-phase approximation diverges at the bifurcation point.

Thus, for describing the bifurcation phenomena under consideration, Magner et al. have developed a periodic-orbit theory free from the divergence [19]. Here I would like to briefly discuss basic ideas of this work.

Since the spheroidal cavity is integrable, we can develop semiclassical method along the line initiated by Berry and Tabor [5]. As usual, we start from the trace integral for the level density in action-angle variables. In the conventional scheme, however, one considers families of orbits with the highest degeneracies (like 3D orbits) but those with lower degeneracies (like equatorial-plane orbits) are not necessarily taken into account. Hence we need to extend the Berry-Tabor approach in order to treat the bifurcation of interest. We thus consider all kinds of stationary points, and calculate (for the lower degeneracy orbits) the integrals over angles, too, by an improved stationary-phase method. "Improved" here means that the trace integrals over both action and angle variables are calculated, as usual, by expanding the exponent of the integrand about the stationary point up to the second order, but the integrations are done within the *finite* physical region as in [5]. If the integration ranges are extended, as usual, to $\pm\infty$, singularity arises in the amplitude, since, at the bifurcation, a stationary point lies just on the edge of the physical integration range. The stationary points need not necessarily lie inside the physical region of integration over the action-angle variables, but they are assumed to be close to the integration limits. In fact, a bifurcation occurs when one of the stationary points crosses the border from the unphysical region (negative values of the action variable) and enter the physical region. As we move away from the bifurcation points, thus obtained contributions from the lower degeneracy orbit families asymptotically approach the results of the conventional stationary-phase approximation.

This approach has been successfully applied to the elliptic billiard model, and it is shown that the bifurcation of the (butterfly-shaped) hyperbolic orbit family from the repeated short-diameter orbit is responsible for emergence of shell structure at large deformations. For instance, it is clearly seen in Fig. 6 that the amplitude of the bifurcating orbit is significantly enhanced in the vicinity of the bifurcation point. Namely, we obtain the maximum instead of the divergence at the bifurcation point. We are now applying this approach to the spheroidal cavity model, and the result will be published in the very near future [19].

7 Concluding remarks

We have discussed quantum manifestations of short periodic orbits and of their bifurcations in the spheroidal cavity, and identified the classical periodic orbits responsible for the emergence of the quantum shell structure at large prolate deformations. Fourier transforms of quantum spectra clearly indicate that 3D periodic orbits born out of bifurcations of the planar orbits in the equatorial plane generate the superdeformed shell structure. A new semiclassical method capable of describing the shell-structure formation associated with these periodic-orbit bifurcations is briefly discussed.

Acknowledgements

I would like to thank the organizing committee of the Nobel Symposium "Quantum Chaos Y2K" for giving me the opportunity to write my view as a discussion leader of one of the sessions on "Description of Quantal Spectra in Terms of Periodic Orbits." The symposium was very stimulating and useful; for instance, it was totally unexpected for me to learn that the periodic-orbit bifurcation in deformed cavities, of the type discussed here, can be used to get high power directional emission from lasers with chaotic resonators. This article is written on the basis of collaborations with Arita et al. [13] and Magner et al. [19].

References

[1] Bohr, A and Mottelson, B.R., "Nuclear Structure" (Benjamin, 1975), vol. 2.

[2] Åberg, S., Flocard, H. and Nazarewicz, W., Ann. Rev. Nucl. Part. Sci. **40**, 439 (1990).

[3] Gutzwiller, M.C., J. Math. Phys. **12**, 343 (1971).

[4] Balian, R. and Bloch, C., Ann. Phys. **69**, 76 (1972).

[5] Berry, M.V. and Tabor, M., Proc. R. Soc. London **A349**, 101 (1976).

[6] Strutinsky, V.M., Magner, A.G., Ofengenden, S.R. and Døssing, T., Z. Phys. **A283**, 269 (1977).

[7] Brack, M. and Bhaduri, R.K., "Semiclassical Physics" (Addison-Wesley, Reading, 1997).

[8] Twin, P.J. *et al.*, Phys. Rev. Lett. **57**, 811 (1986).

[9] Lermé, J., Bordas, Ch., Pellarin, M., Baguenard, B., Vialle, J.L. and Broyer, M., Phys. Rev. **B48**, 9028 (1993).

[10] Arita, K. *et al.*, to be published.

[11] Misu, T. *et al.*, to be published.

[12] Nishioka, H., Ohta, M. and Okai, S., Mem. Konan Univ., Sci. Ser. **38**(2), 1 (1991).

[13] Arita, K., Sugita, A. and Matsuyanagi, K., Prog. Theor. Phys. **100**, 1223 (1998).

[14] Frisk, H., Nucl. Phys. **A511**, 309 (1990).

[15] I would like to point out that they appear through bifurcations also for irrational ratios, if anharmonic terms like octupole deformations are added; see [20–22]. I also like to mention that there is an analogous open problem concerning the semiclassical origin of the left-right asymmetry in nuclear shapes [23].

[16] Nolan, P.J. and Twin, P.J., Ann. Rev. Nucl. Part. Sci. **38**, 533 (1988).

[17] Janssens, R.V.F. and Khoo, T.L., Ann. Rev. Nucl. Part. Sci. **41**, 321 (1991).

[18] *Berkeley Isotope Project Data File*, http://isotopes.lbl.gov/isotopes/sd.html.

[19] Magner, A.G., Fedotkin, S.N., Arita, K., Misu, T., Matsuyanagi, K., Schachner, T. and Brack, M., Prog. Theor. Phys. **102**, 551 (1999), and to be published.

[20] Arita, K. and Matsuyanagi, K., Prog. Theor. Phys. **91**, 723 (1994).

[21] Arita, K. and Matsuyanagi, K., Nucl. Phys. **A592**, 9 (1995).

[22] Heiss, W.D., Nazmitdinov, R.G. and Radu, S., Phys. Rev. **B51**, 1874 (1995).

[23] Sugita, A., Arita, K. and Matsuyanagi, K., Prog. Theor. Phys. **100**, 597 (1998).

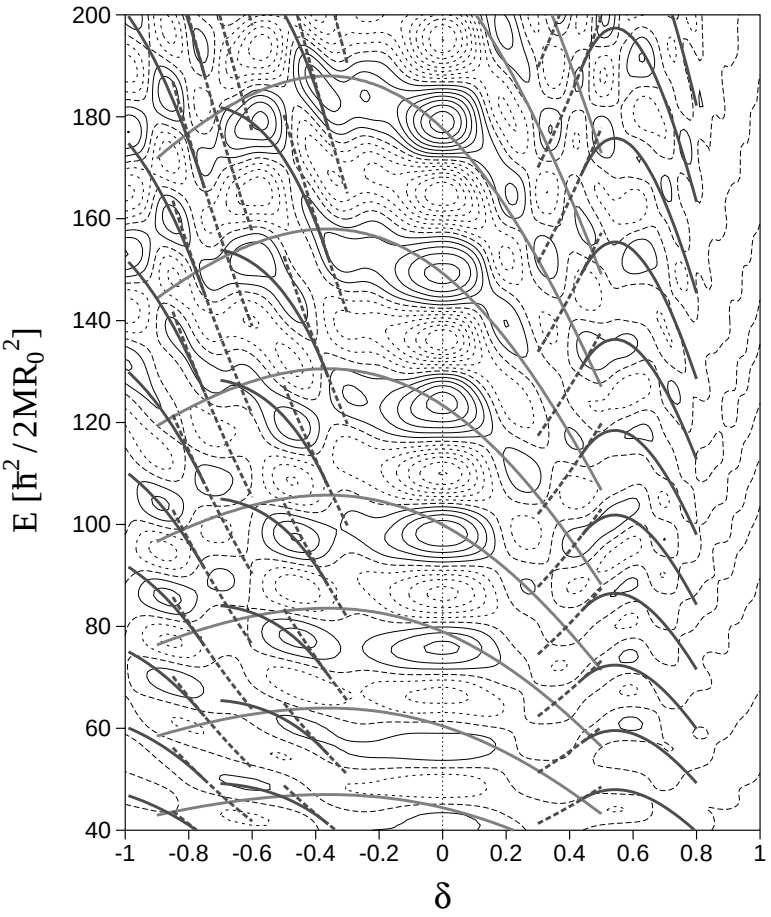

Figure 2: Oscillating part of the smoothed level density displayed as a function of the energy (in unit of $\hbar^2/2MR_0^2$) and deformation parameter δ. Here M and R_0 denote the mass of the particle and the radius at the spherical shape, respectively. The deformation parameter δ is related to the axis ratio $\eta \equiv a/b$ by $\delta = 3(\eta-1)/(2\eta+1)$ in the prolate case discussed in the text. Solid, dashed and dotted contour curves correspond to negative, zero and positive values, respectively. Constant-action lines for important periodic orbits are indicated by thick solid and broken lines (see text). This figures is taken from [13].

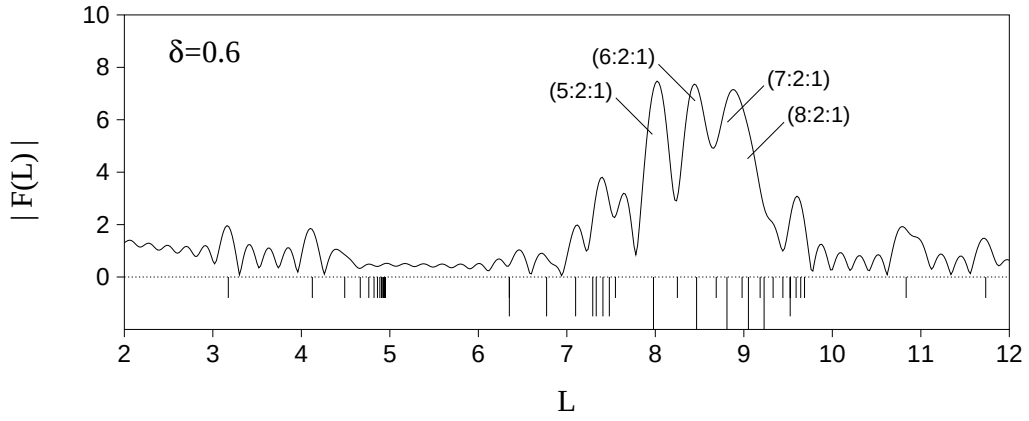

Figure 3: Length spectrum (Fourier transform of quantum level density) for the spheroidal cavity with $\delta = 0.6$ (axis ratio 2:1). At the bottom, the lengths (in unit of R_0) of classical periodic orbits are indicated by vertical lines. Long, middle and short vertical lines are used for 3D orbits, planar orbits in the meridian, and planar orbits in the equatorial planes, respectively. This figures is taken from [13].

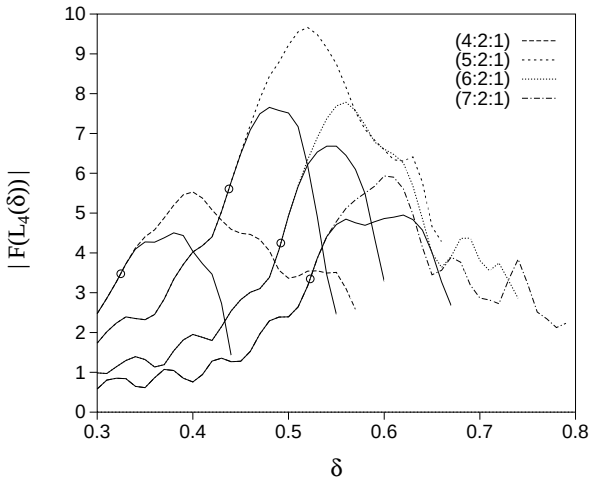

Figure 4: Deformation dependence of the Fourier amplitudes defined in Eq. (3), at lengths $L = L_r$ of the butterfly-shaped hyperbolic orbit (4:2:1) in the meridian plane and of 3D orbits (p:2:1). Solid curves correspond to those for equatorial-plane orbits from which these orbits are bifurcated. This figures is taken from [13].

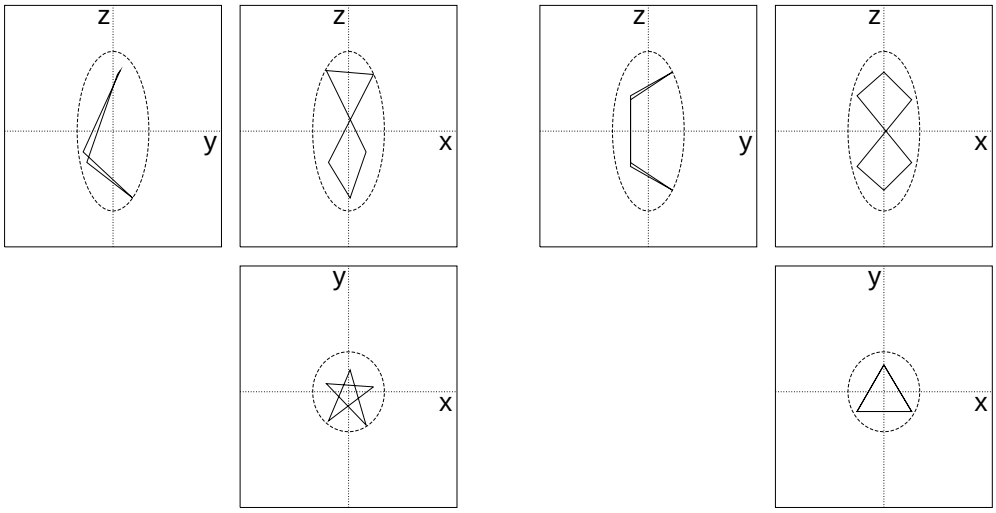

Figure 5: Three-dimensional orbits (5:2:1) and (6:2:1) in the superdeformed prolate cavity (axis ratio $\eta = 2$). Their projections on the (x, y), (y, z) and (z, x) planes are displayed. This figures is taken from [13].

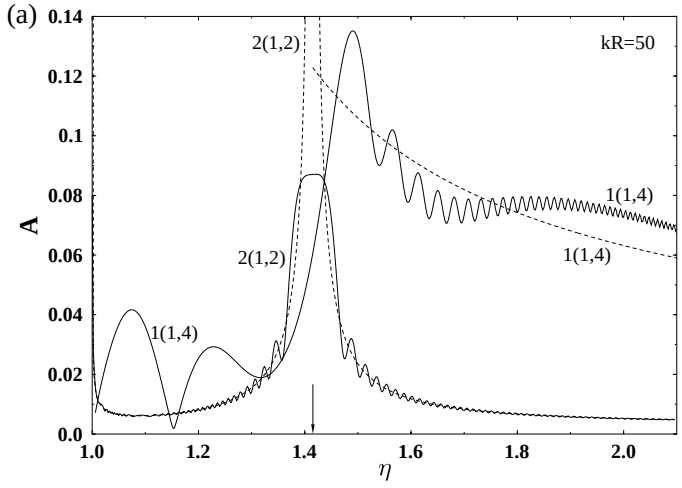

Figure 6: Deformation dependence of the amplitudes A for the second repetition of the short diameter 2(1,2) and the butterfly orbits 1(1,4) in the elliptic billiard, calculated at $kR_0 = 50$ by the improved stationary-phase method of Ref. [19]. Their absolute values are drawn by solid curves as functions of the axis ratio η. For comparison, standard results of the extended Gutzwiller trace formula are plotted by short-dashed curves. This figure is taken from [19].